

UDC 681.5 (045)

<sup>1</sup>V. V. Chikovani,  
<sup>2</sup>H. V. Tsiruk**SHOCK RESISTANCE OF DIFFERENTIAL TYPE RING-LIKE RESONATOR VIBRATORY GYROSCOPE**

Institute of Air Navigation, National Aviation University, Kyiv, Ukraine

<sup>1</sup>[valeriy-chikovani@rambler.ru](mailto:valeriy-chikovani@rambler.ru), <sup>2</sup>[annylee@ukr.net](mailto:annylee@ukr.net)

**Abstract**—This work presents investigation of differential Coriolis vibratory gyroscope ability to external shock suppression. First of all pulse amplitude in voltage caused by external mechanical shock of 100 g is estimated for the two sensor designs. Then, using differential Coriolis vibratory gyroscope Simulink model, output signals of two measurement channels are analyzed. It is shown that differential Coriolis vibratory gyroscope damps amplitude of erroneous angle rate caused by shock directed along sensing axis of no less than 3 times in comparison with non differential Coriolis vibratory gyroscope. Influence of lateral shock is also analyzed.

**Index Terms**—Differential Coriolis vibratory gyroscope; shock; error angle rate.

**I. INTRODUCTION**

Differential Coriolis vibratory gyroscope (D-CVG) using metallic cylindrical resonator was firstly presented in [1] and in more detail was considered in [2]. It gives signals from two channels whose difference increases rate information two times and compensates for the bias components which are equal for two channels. Sum of these two channels under proper tuning can compensate for the angle rate measured and gives bias components information during rate measurements. This bias information can be used, as noted in [2], to correct bias components in the fist, difference channels signal, to increase measurement accuracy that results in more accurate navigation and attitude parameters determination.

Navigation systems as a rule experience shocks when measuring angle rate that results in erroneous angle rate. During external mechanical shock along sensing axis, in accordance with cylindrical resonator design, all drive and sense electrodes simultaneously experience deformations resulting in voltage pulses in all four control circuits and, as a result, in erroneous angle rate in each of two measurement channels. These erroneous angle rates are almost equal for two channels and their difference signal reduces error in angle rate caused by external mechanical shock.

Pulse amplitude in voltage caused by mechanical shock is estimated for two sensor designs. Resultant error angle rate on the output of the difference channel is calculated using computer simulation based on D-CVG Simulink model and is compared with that of non differential rate CVG.

**II. SENSOR DESIGNS**

The two types of cylindrical sensors are considered in this section to estimate pulse amplitude in

voltage caused by external mechanical shock. First design is the cylinder made of nickel alloy with thicker, than rest of the cylinder, rim and piezoceramic plates as electrodes glued on its bottom as depicted in Fig. 1 [3].

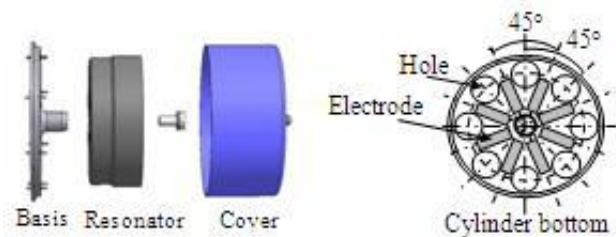


Fig. 1. First type sensor with electrodes on the cylinder bottom

In the second type sensor the electrodes are glued on the lower part of the cylinder wall as depicted in Fig. 2 [4].

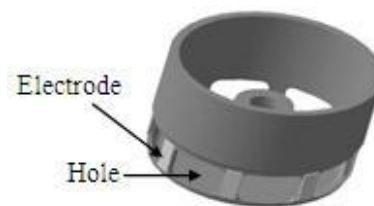


Fig. 2. Second type sensor with electrodes on the cylinder wall

**III. SHOCK PULSE ESTIMATION IN VOLTAGE**

Suppose that the external mechanical shock of rectangular form (worst case), 2 ms duration and 100 g amplitude is acting along the CVG sensing axis in the process of CVG operation. Under action of such shock the bottom of the first type resonator together with piezoelectrodes are deformed and voltages are picked off from all eight piezoelectrodes in the form of shock pulse. The resonator bottom fixed in its

center is deformed due to the force acting from the massive rim (see Fig.1, left). Mass of the rim is determined as production of its volume by material density

$$m = 2\pi r h t_r \rho, \quad (1)$$

where  $r$ ,  $h$ ,  $t_r$ ,  $\rho$  are the rim's radius, height, thickness and material density, respectively. Under action of the 100 g shock the rim's weight increases and bottom experiences total force equal to

$$F = 100mg = 200\pi r h t_r \rho g. \quad (2)$$

Each of eight electrodes glued on the spokes, formed between holes (see fig.1, right), is subjected to the action of the force equal to  $F_p = F/8 = 25\pi r h t_r \rho g$  and is deformed by thickness. Spoke's strain  $\varepsilon(x)$  distribution along its longitudinal coordinate  $x$  is [4]

$$\varepsilon(x) = \frac{6F_p(L_s - x)}{E_s w_s t_s^2}, \quad (3)$$

where  $L_s$ ,  $E_s$ ,  $w_s$ , and  $t_s$  are spoke's length, Young's modulus, width and thickness, respectively. As a result of this deformation together with piezoelectrode that has the spoke's length and width and capacitance  $C_p$ , voltage,  $V_1$  is induced [6]

$$V_1 = \frac{d_{31} E_p w_p}{C_p} \int_0^{L_s} \varepsilon(x) dx, \quad (4)$$

where  $d_{31}$  is piezoelectric charge constant.

Substitution of expressions (3) in (4) and integration yields

$$V_1 = \frac{75d_{31}\pi r h t_r \rho g E_p L_s^2}{C_p E_s t_s^2} F_p. \quad (5)$$

For real sensor the following parameter values can be realized:  $d_{31} = 1.09 \cdot 10^{-10}$  C/N,  $r = 12.5$  mm,  $h = 10$  mm,  $t_r = 1$  mm,  $\rho = 7.8 \cdot 10^3$  kg/m<sup>3</sup>,  $L_s = 4$  mm,  $C_p = 800$  pF,  $t_s = 0.4$  mm,  $E_p = 4 \cdot 10^{10}$  N/m<sup>2</sup>,  $E_s = 20 \cdot 10^{10}$  N/m<sup>2</sup>. After calculations the output pulse in voltage caused by external mechanical shock for the first type sensor, presented in Fig. 1, is  $V_1 \approx 4.5$  V. Since the diametrically opposite electrodes are connected with each other this pulse in voltage increases 2 times and takes the value  $V_{1\Sigma} \approx 9$  V.

For the second type sensor force  $F_p$  caused by shock will squeeze the spoke along its length. In this case strain is

$$\varepsilon = \frac{F_p}{k_s^l L_s}; \quad k_s^l = \frac{E_s w_s t_s}{L_s}, \quad (6)$$

where  $k_s^l$  is spoke's longitudinal rigidity.

As result of spoke compression together with piezoelectrode, the pulse in voltage  $V_2$  is

$$V_2 = \frac{d_{31} E_p w_p}{C_p} \varepsilon L_s = \frac{25d_{31}\pi r h t_r \rho g E_p L_s}{C_p E_s t_s}. \quad (7)$$

Calculations with the same parameters gives for the second type sensor, presented in Fig. 2, shock pulse in voltage equal to  $V_2 \approx 0.2$  V, hence, sensor will send to the standing wave control system pulse in voltage equal to  $V_{2\Sigma} \approx 0.4$  V. As can be seen for the second type sensor voltage pulse caused by external mechanical shock along sensing axis is about 20 times less than that of for the first type one.

As to lateral shock both type sensor have equal ability to suppress it. Really, diametrically opposite electrodes, which are short-circuited, deform so that they generate different polarity charges and in the first approximation compensate for each other.

### III. DIFFERENTIAL CVG MODEL

Differential Coriolis vibratory gyroscope model consists of sensor model and standing wave control system model. The former is described by well-known dynamic equations of two dimensional pendulum [6]

$$\begin{aligned} \ddot{x} - 2k\Omega \dot{y} + d_{xx} \dot{x} + d_{xy} \dot{y} + k_{xx} x + k_{xy} y &= f_x; \\ \ddot{y} - 2k\Omega \dot{x} + d_{yx} \dot{x} + d_{yy} \dot{y} + k_{yx} x + k_{yy} y &= f_y, \end{aligned} \quad (8)$$

where  $k$  is Brian coefficient,  $d_{xx} = 2/\tau + \Delta(1/\tau)\cos\theta_\tau$  is  $X$  axis damping coefficient,  $2/\tau = 1/\tau_1 + 1/\tau_2$ ,  $\Delta(1/\tau) = 1/\tau_1 - 1/\tau_2$  where  $\tau_1$  is minimum resonator's damping time,  $\tau_2$  is maximum resonator's damping time,  $d_{xy} = \Delta(1/\tau)\sin\theta_\tau$  is damping cross-coupling,  $k_{xx} = \omega^2 - \omega\Delta\omega\cos 2\theta_\omega$  is normalized by mass resonator rigidity along  $X$  axis,  $\omega\Delta\omega = (\omega_1^2 - \omega_2^2)/2$ , where  $\omega_1$ ,  $\omega_2$  are maximum and minimum resonant frequency,  $k_{xy} = -\omega\Delta\omega\sin 2\theta_\omega$  is rigidity cross-coupling,  $d_{yy} = 2/\tau - \Delta(1/\tau)\cos\theta_\tau$  is  $Y$  axis damping coefficient,  $d_{yx} = d_{xy}$ ,  $k_{yy} = \omega^2 + \omega\Delta\omega\cos 2\theta_\omega$  is resonator rigidity along  $Y$  axis normalized by mass,  $k_{yx} = k_{xy}$ ,  $f_x$  and  $f_y$  are normalized by mass control forces,  $\theta_\omega$  is angle between minimum frequency axis and standing wave (antinode) axis,  $\theta_\tau$  is angle between minimum damping axis and standing wave (antinode) axis.

Standing wave control system block diagram is presented in Fig. 3 [2].

It consists of two drive and two sense channels  $X$  and  $Y$ . Two drive channels excite standing wave so that it is located between the electrodes. In this case two sense channels, when there is rotation, carry

information about  $\Omega$  ( $X$  channel) and  $-\Omega$  ( $Y$  channel) angle rates. Under the proper tuning sum of two sense channels,  $z_x+z_y$ , has not information about angle rate, but carry information about bias components. The difference,  $z_x-z_y$ , has information of  $2\Omega$  and bias components which were not compensated for [2].

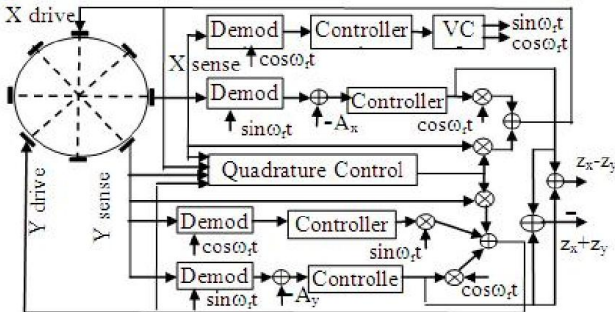


Fig. 3. Differential Coriolis vibratory gyroscope control system block diagram

IV. COMPUTER SIMULATION RESULTS

Figure 4 shows transient process after mechanical shock 100 g, 2 ms duration along sensing axis of the first type CVG which causes 9 V pulse in voltage after 100 g, 2 ms shock for the first type sensor over all four drive and sense CVG channels. Curve 1 in fig.4 depicts pulse in voltage converted into angle rate using CVG scale factor, curves 2 and 3 depict non D-CVG and D-CVG transient processes, respectively. As can be seen from this figure D-CVG damps shock about 5 times more in comparison with non D-CVG.

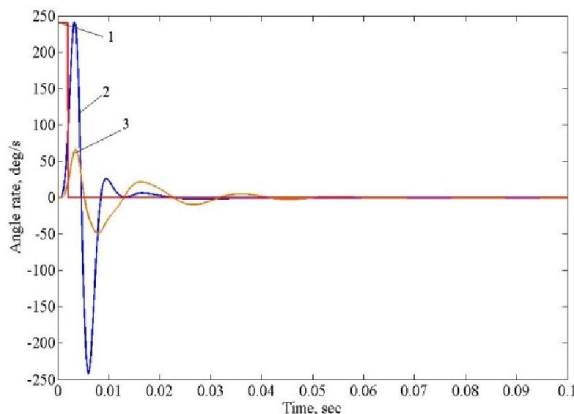


Fig. 4. Non D-CVG (2) and D-CVG (3) transient processes after 100 g, 5 ms shock for the first type sensor

Figure 5 shows transient processes when shock duration is 5 ms.

As can be seen from Fig. 5 growth in shock pulse duration results in increasing both CVGs responses. D-CVG transient process duration, described by curve 3, is more than non D-CVG. This can be explained by different tuning parameters of  $X$  and  $Y$  channels of D-CVG, such as bandwidth, phase dif-

ference etc. Nevertheless, differential CVG damps shock about 4 times more than that of non D-CVG.

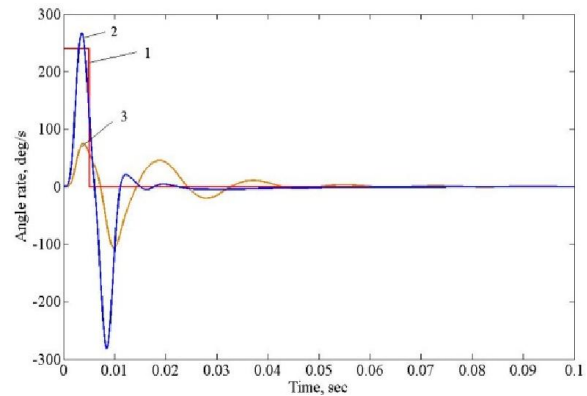


Fig. 5. Non D-CVG (2) and D-CVG (3) transient processes after 100 g, 5 ms shock for the first type sensor

Figure 6 shows transient processes of non D-CVG and D-CVG for the second type sensor, presented in Fig. 2, for mechanical shock 100 g amplitude and 5 ms duration along sensing axis.

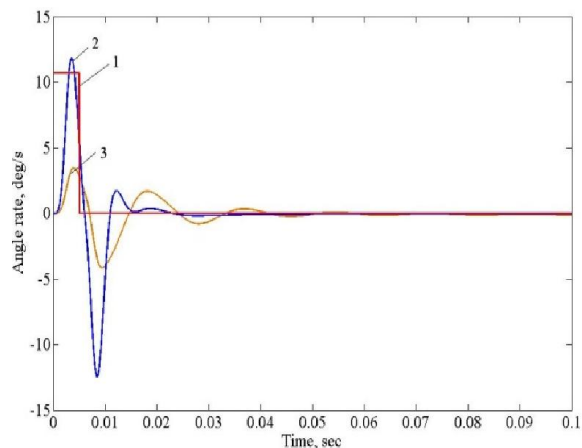


Fig. 6. Non D-CVG and D-CVG transient processes after 100 g, 5 ms shock for the second type sensor

This figure shows that behavior of transient process for the second type sensor is the same as for the first type one, but second type sensor amplitude is about 20 times less than that of the first type one. D-CVG response amplitude is about 3.5 times less than that of the non D-CVG for the second type sensor.

Despite of lateral shock can be compensated in the first approximation it will be useful to show D-CVG behavior when there is no full compensation for the lateral shock.

Figure 7 shows transient process after 1 V of non compensated voltage shock in  $Y$  sense channel.

Shock starting time is 0.7 s. The same result can be obtained for lateral shock along  $X$  sense axis.

As to shock acting along  $X$  and  $Y$  drive axes it should be noted that there are no responses on the output signal when shock duration is in interval

1–5 ms because resonator, as a band pass filter, rejects such disturbances.

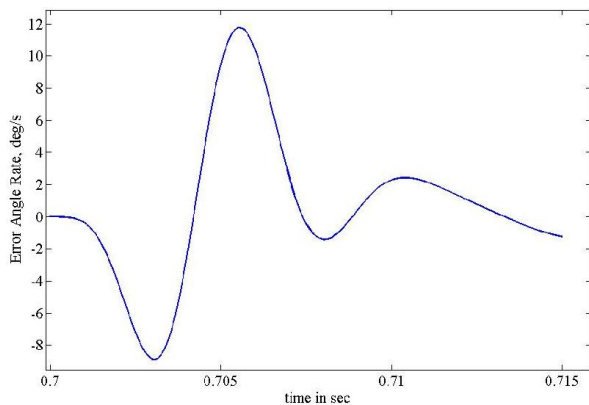


Fig. 7. Differential Coriolis vibratory gyroscope transient process after 1 V, 2 ms lateral shock

Figure 8 shows shock response of  $X$  and  $Y$  channels difference frequency, which quadrature control unit, shown in D-CVG block diagram of Fig. 3, is responsible for.

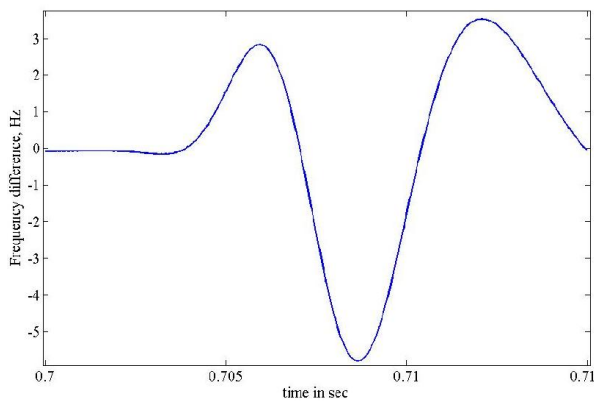


Fig. 8. Differential Coriolis vibratory gyroscope transient process after 1 V, 2 ms lateral shock along Y sense axis

As can be seen from Fig. 8 maximum deviation is about 6 Hz and duration of transient process is about 0.01 s.

## CONCLUSION

Differential CVG has more than 3 times higher mechanical shock damping capacity in comparison with non differential CVG, for the both type sensors.

The second type sensor, presented in Fig. 2, with electrodes and holes on cylinder wall has 20 times higher shock suppression along sensing axis in comparison with the first type one.

## REFERENCES

- [1] Chikovani, V. V.; Umakhanov, E. O.; Marusyk, P. I. "The compensated differential CVG." *Gyro Technology: Symposium*, 16-17 September 2008. Germany: Karlsruhe university. pp. 3.1-3.8.
- [2] Chikovani, V. V.; Suschenko, O. A. "Differential mode of operation for ring-like resonator CVG." *IEEE Proc. Intern. Conf. on Electronics and Nanotechnology (ELNANO)*, NTUU KPI, Kyiv, Ukraine, 15-18 April, 2014, pp.451–455.
- [3] Yatsenko, Yu. A.; Chikovani, V. V.; Kovalenko, V. A. "Cylindrical sensing element for Coriolis vibratory gyroscope." *Patent#79166 Ukraine*, Int.cl. G01C 19/56. # a 2005 05177; Appl. 31.05.2005; Publ. 15.12.2006, Bull. # 7, 7 p. (in Ukrainian).
- [4] Petrenko, O. V. "Design analysis and parameters choice of metallic cylindrical resonator sensor for Coriolis vibratory gyroscope." *Electronics and control systems*, no. 3 (41), NAU, Kyiv, 2014, pp. 101–105.
- [5] Haifeng Dong "Design and Analysis of a MEMS Comb Vibratory Gyroscope." *Thesis, Master of Science*, Bridgeport University, April 2009, 119 pp.
- [6] Reza, S. O. Moheimani, Andrew J. Fleming "Piezoelectric Transducers for Vibration Control and Damping." *Springer*, 2006, 256 p.
- [7] Lynch, D. D. "Coriolis vibratory gyros." *Proc. Gyro Technology Symposium*, 21-23 Sept., 1998, Stuttgart, Germany, pp. 3.1–3.14.

Received 24 October 2014.

**Chikovani Valeriy**. Doctor of Engineering. Member of IEEE.

Education: Moscow Physical-Technical Institute, Moscow, USSR (1975).

Research interests: gyroscopy, inertial navigation system, control systems and digital information processing.

Publications: 90.

E-mail: [v\\_chikovani@ukr.net](mailto:v_chikovani@ukr.net)

**Tsiruk Hanna**. Student.

Education: National Aviation University pre-magister.

Research interests: gyroscopy, control systems.

Publications: 4.

E-mail: [annylee@ukr.net](mailto:annylee@ukr.net)

**В. В. Чіковані, Г. В. Цірук. Ударостійкість вібраційного гіроскопа диференційного типу з кільцевим резонатором**

Досліджено здатність коріолісового гіроскопа диференційного типу до придушення зовнішнього удару. Розраховано амплітуди імпульсів напруги викликані зовнішнім механічним ударом у 100 г для двох конструкцій

чутливого елементу. Проаналізовано вихідні сигнали двох його вимірювальних каналів використовуючи Simulink модель диференційного коріолісового гіроскопа. Показано, що диференційний коріолісовий гіроскоп гасить амплітуду помилкової кутової швидкості, викликаної ударом спрямованим вздовж осі чутливості не менш ніж 3 рази в порівнянні з не диференційним коріолісовим гіроскопом. Проаналізовано вплив бокового удару.

**Ключеві слова:** диференційний гіроскоп; удар; помилкова кутова швидкість.

**Чиковані Валерій Валеріанович.** Доктор технічних наук. Член IEEE.

Освіта: Московський фізико-технічний інститут, Москва, Росія (1975).

Напрямок наукової діяльності: гіроскопи, інерційні навігаційні системи, системи управління та цифрова обробка інформації.

Кількість публікацій: 90.

E-mail: [v\\_chikovani@ukr.net](mailto:v_chikovani@ukr.net)

**Цірук Ганна Вікторівна.** Студентка.

Освіта: Національний авіаційний університет, Київ, Україна.

Напрямок наукової діяльності: гіроскопи, системи управління.

Кількість публікацій: 4.

E-mail: [annylee@ukr.net](mailto:annylee@ukr.net)

**В. В. Чиковани, Г. В. Цірук. Удароустойчивость вибрационного гироскопа дифференциального типа с кольцевым резонатором**

Исследована способность кориолисова гироскопа дифференциального типа к подавлению внешнего удара. Рассчитаны амплитуды импульсов напряжения вызванной внешним механическим ударом в 100 g для двух конструкции чувствительного элемента. Проанализированы выходные сигналы двух его измерительных каналов используя Simulink модель дифференциального кориолисова гироскопа. Показано, что дифференциальный кориолисовый гироскоп гасит амплитуду ложной угловой скорости, вызванной ударом направленным вдоль оси чувствительности не менее 3 раза по сравнению с не дифференциальным кориолисовым гироскопом. Проанализировано влияние бокового удара.

**Ключевые слова:** дифференциальный гироскоп; удар; погрешность угловой скорости.

**Чиковани Валерій Валеріанович.** Доктор технических наук. Член IEEE.

Освіта: Московский физико-технический институт, Москва, Россия (1975).

Направление научной деятельности: гироскопы, инерциальные навигационные системы, системы управления и цифровая обработка информации.

Количество публикаций: 90.

E-mail: [v\\_chikovani@ukr.net](mailto:v_chikovani@ukr.net)

**Цірук Ганна Вікторівна.** Студентка.

Образование: Национальный авиационный университет. Киев. Украина.

Направление научной деятельности: гироскопы, системы управления.

Количество публикаций: 4.

E-mail: [annylee@ukr.net](mailto:annylee@ukr.net)